

Journal of Materials Chemistry A

Accepted Manuscript



This is an *Accepted Manuscript*, which has been through the Royal Society of Chemistry peer review process and has been accepted for publication.

Accepted Manuscripts are published online shortly after acceptance, before technical editing, formatting and proof reading. Using this free service, authors can make their results available to the community, in citable form, before we publish the edited article. We will replace this *Accepted Manuscript* with the edited and formatted *Advance Article* as soon as it is available.

You can find more information about *Accepted Manuscripts* in the [Information for Authors](#).

Please note that technical editing may introduce minor changes to the text and/or graphics, which may alter content. The journal's standard [Terms & Conditions](#) and the [Ethical guidelines](#) still apply. In no event shall the Royal Society of Chemistry be held responsible for any errors or omissions in this *Accepted Manuscript* or any consequences arising from the use of any information it contains.

Microwave plasma-induced graphene-sheet fibers from waste coffee grounds

Received 00th January 20xx,
Accepted 00th January 20xx

DOI: 10.1039/x0xx00000x

www.rsc.org/

Zhipeng Wang^{*a,b}, Hironori Ogata^{c,d}, Shingo Morimoto^a, Masatsugu Fujishige^a, Kenji Takeuchi^a, Hiroyuki Muramatsu^b, Takuya Hayashi^b, Josue Ortiz-Medina^a, Mohd Zamri Mohd Yusop^{e,f}, Masaki Tanemura^e, Mauricio Terrones^g, Yoshio Hashimoto^{a,b} and Morinobu Endo^a

Graphene-sheet fiber, a novel structure of graphitic carbon, grows from coffee grounds under the condition of microwave plasma irradiation. The resulting fiber consisting of only few-layer graphene without hollow structure inside possesses a large amount of graphene edges and high conductivity. Duet to these advantages, graphene-sheet fibers may be find applications in the electrochemical energy conversion and storage.

Graphene is a two-dimensional hexagonal crystal lattice consisting of a single layer of sp²-bonded carbon atoms.¹ Graphitic carbons, from common graphite, fullerenes,² carbon nanotubes,³ filamentous graphite⁴ to carbon nanowalls⁵ and graphene nanoribbons,^{6,7} which are regarded to be formed by the assembly of hexagonally atomic graphene under the conditions of defects, rolled up, twisted or paralleled each other, have led to much speculation of carbon materials in theory and applications due to their special and excellent properties. Buckminster fullerenes² and carbon nanotubes³ were formed initially on the opposite electrodes by arc vaporization of carbonaceous materials, e.g. graphite. To scale up their production for industrial applications, carbon nanotubes in large amounts could be achieved by chemical vapor deposition of hydrocarbons with a metal catalytic assist or directly over on a catalytic metal surface, which has been also used to fabricate carbon fibers,⁸ graphite filaments,⁴ and graphene films.⁹⁻¹¹ With the development and utilization of plasma technique, the growth of carbon nanotubes¹² and graphene^{13, 14} can be realized at low temperatures and the graphitic carbon families have been further expanded, such as the synthesis of carbon nanowalls,⁵ and graphene nanosheets.^{15,16} Interestingly, plasma-matter interaction to synthesize graphitic carbon with various morphologies and microstructures can achieved from not only carbonaceous gases but also other precursors, such as butter, cheese, honey, honeycomb, and waste carbon black.¹⁷⁻²¹ Here we report that graphene-sheet fiber (GSF), a novel form of graphitic carbon and is composed of few-layer graphene which grow coaxially, can be produced by microwave plasma irradiation (MPI) of waste coffee grounds without any special treatment or the use of additional reagent. Transmission electron microscope images show that no cylindrically hollow structure exists inside GSFs, suggesting that the new form is not graphene-decorated carbon nanotubes (graphenated carbon nanotubes).²² The GSFs have demonstrated good electrical conductivity and high specific capacitance. Thus, it has been speculated that GSFs can be utilized as electrodes for electrochemical energy conversion and storage with great performances.

Figure 1a shows a schematic diagram of MPI technique for the coffee-ground-derived nanocarbons. Prior to plasma generation, the base pressure of the chamber was evacuated to be about 1 Torr. Subsequently, a hydrogen-argon gas mixture (1:1) was introduced into the reaction chamber, and then was ignited by 2.45 GHz microwave at 900 W to produce the mixture plasma. After the bombardment of plasma for 15 min, the waste coffee grounds loaded in a nickel foil case (nickel foil: 0.02 mm in thickness) were carbonized with oil extraction on the quartz tube and some black materials including GSFs were formed on the surface of the nickel case near to microwave entrance. The resulting black materials were investigated using a Hitachi SU8000/8020 scanning electron microscopy (SEM), a JEM2100 aberration-corrected transmission electron microscopy (TEM, electron energies of 80 keV), electron dispersive X-ray analyzer (EX-64175JNU) attached in JSM-7000F, and an inVia Renishaw Raman spectroscopy (laser wavelength of 532 nm, ×100 objective lens). The GSF of varying lengths and diameters convolved on the surfaces of other carbon materials. The deposited nickel surface also contained carbon nanotubes (with and without graphene sheets on their sides) within the range of 10-200 nm diameter, and the carbon particles with 0.1-5 μm diameter, which were also composed of few-layer graphene grown in the radial direction.

Figure 1b shows a representative high-magnification SEM image of a part of individual fiber (see Figure S1, ESI†), which consists of wavy sheets with various sizes. Energy dispersive X-ray analysis confirmed only carbon and oxygen elements in the fiber (Figure S2,

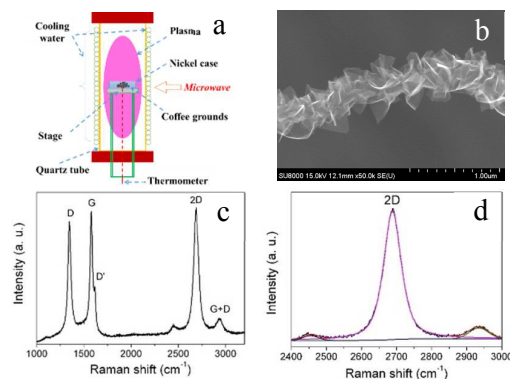


Figure 1 A schematic diagram of our experiment, and morphology and microstructure of individual GSF obtained from waste coffee grounds by MPI technique. (a) Setup of MPI technique. (b) SEM image of GSF. (c) Raman spectrum obtained at the laser of 532 nm. (d) 2D peak in Raman spectrum fitted by a single Lorentzian.

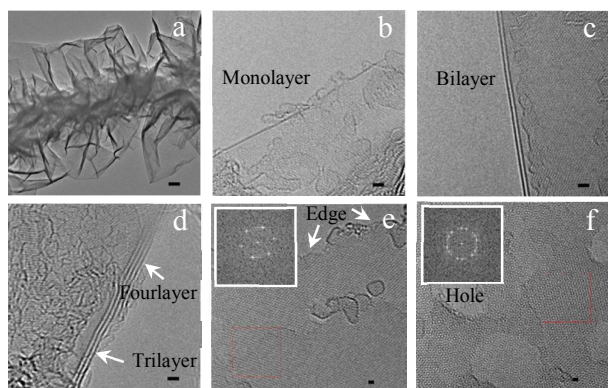


Figure 2 TEM images of individual GSF. (a) Graphitic fiber without hollow structure consists of graphene nanosheets with varying thickness. (b) Monolayer graphene. (c) Bilayer graphene. (d) Tri- and four-layer graphene. (e) High-resolution TEM image from monolayer graphene. Inset: a hexagonal pattern of carbon atoms by fast Fourier transform for monolayer graphene. (f) High-resolution TEM image from few-layer graphene. Inset: a dotted ring pattern for few-layer graphene. Scale bars: 50 μm in a, 1 nm in b-d, and 0.5 nm in e-f.

Cu signal ascribes to the copper mesh grid. A typical Raman spectrum of the fiber with about 800 nm diameter is shown in Figure 1c. There are three main pronounced peaks in this spectrum which located at 1347 cm^{-1} for D peak, 1578 cm^{-1} for G peak, and 2688 cm^{-1} for 2D peak, respectively. The intensity ratio of 2D peak to G peak is about 1.7 and the full-width at half-maximum of the 2D peak is about 60 cm^{-1} as well as the single Lorentzian bandwidth of 2D peak (Figure 1d) is similar to that of monolayer graphene, suggesting that these sheets are made of few-layer graphene with turbostratic stacking.²⁴ The intensity ratio of D peak to G peak is about 1.1 and the D' peak around 1616 cm^{-1} appears, implying that the few-layer graphene in the fibers have a large amount of open edges.

High-resolution TEM observations are useful and direct to identify the atomic structures of graphene sheets including their real layer number, stacking configuration, crystalline degree, topological defects and edges. For our samples, we found that the sheets of the fiber consist of from mono-, bi-, and tri-layer to few layer graphene (Figure 2b-d). The distance of layer to layer was in the range of 0.345-0.352 nm, which is slightly greater than d_{002} spacing of graphite (0.335 nm). We can observe that the graphene sheets possess edges (Figure 2e), nanoholes (Figure 2f), and topological defects in their surfaces (Figure 2f). The observed defects located along the grain boundaries are non-hexagonal rings (such as, pentagonal and heptagonal rings). We also observed that a hexagonal pattern of carbon atoms was obtained by fast Fourier transform for monolayer graphene (Figure 2e), and a dotted ring pattern for few-layer graphene with turbostratic structure (Figure 2f). The fast Fourier transform results display our samples have high crystallinity under the conditions of the plasma irradiation. The TEM results which are related to the growth of relatively crystalline graphene with plenty of edges and stacked layers are consistent with our mentioned-above Raman analyses.

TEM image in Figure 2a verifies that the GSFs are not hollow, which are different from graphenated carbon nanotubes that were usually synthesized from the dissociation of hydrocarbon gas using plasma-enhanced chemical vapor deposition.²² Figure 3a shows an overview of GSFs with various lengths and diameters on carbon particles. Most of GSFs were 300-500 μm in length and 0.3-2 μm in diameter (Figure 3a-c). The diameter of the smallest fiber we observed was about 30 nm (Figure 3d). It seems that the smallest fiber comprised of individual sheets linked one after another, which resemble twisted graphene ribbons with various shapes and behaviors.²⁵ As mentioned above, accompanying GSF growth,

other nanocarbons including carbon nanotubes, graphenated carbon nanotubes, and particle-like carbon (Figure 3e-f) can be also formed on the nickel substrate, which were confirmed by TEM images (see Figure S3). Based on the analyses of rice husk (RH)-derived nanocarbons by MPI technique, nanotubes and graphene structures strongly depend on the experimental parameters, such as temperature and pressure.²⁶ Thus, these resulting structures obtained here are helpful to understand the GSF growth under the irradiation of coffee grounds by microwave plasma.

To understand the growth of our samples, we used this method to irradiate the waste coffee grounds with different experimental parameters. Petal-like sheets and spherical carbon onions were achieved by argon plasma under the same condition. In this case, however, the fiber-like samples are not available, indicating that hydrogen plays a decisive role in the growth of GSFs. Compared to few-layer graphene nanosheets from plasma-assisted deposition of hydrocarbon,¹⁶ solid carbon,²¹ and Kapton polyimide,²⁷ we observed that the growth of GSFs also need higher deposition temperature and pressure, which are compatible with the formation of graphitic sheets on the side walls of carbon fibers on wet-etched nickel foils.²⁸ We analyzed the chemical composition of different parts of some individual GSFs that were transferred on the copper grid mesh. Except for copper, no metal signal can be detected in our fibers (Figure S2). However, we can find that our carbon nanotubes and graphenated carbon nanotubes encapsulate nickel particles inside. Careful scanning electron microscope observations show that the graphitic fibers lay on both carbon nanotubes and particles, which grew on the nickel surface at different conditions of pressure and temperature. Consequently, we infer a possible growth model of GSFs as follows: During the irradiation of microwave hydrogen and argon plasma, waste coffee grounds which mainly contain lignin, cellulose and hemicellulose become biochar, and produce carbon atoms. The process of carbonization of coffee grounds involves the extraction of bio-oil and the emission of some biogases (H_2 , CH_4 , CO , CO_2 , et al.), which can cause the increase of the deposition pressure. Under the condition of plasma, carbon atom deposits lead to spherical particles with the energetic dangling bonds. Prior to the formation of carbon layer, the surface of nickel foil should be modified to product nickel particles by the bombardment of plasma. Similar to the RH-derived nanocarbons,²⁶ with increasing temperature and pressure, the carbon nanotubes can be formed with the assist of nickel particles. Subsequently, the pressure decreases but the temperature increase. The carbon particles consisting of few-layer graphene grew on the surface of carbon nanotubes and nickel foil because their growth is independent of substrates. Thus, we observed many kinds of structures including carbon nanotubes (with and without graphene sheets on their sidewalls) and particle-like graphene on the nickel

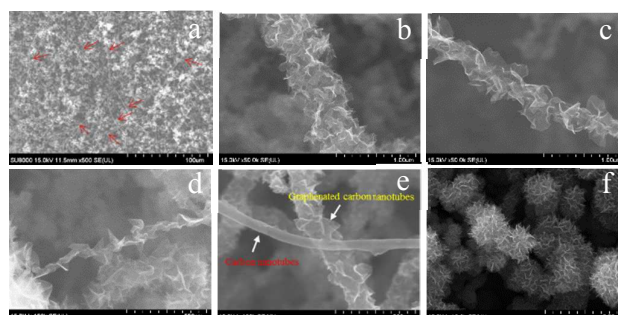


Figure 3 Morphologies of graphene-based carbon materials from waste coffee grounds. (a)-(f), SEM images. (a) Some GSFs grown on the surface of particle-like carbons. Indicated by red arrows. (b)-(d) Individual GSFs with various diameters. The smallest fiber we observed with 30 nm diameter shown in (d). (e) Carbon nanotubes and graphenated carbon nanotubes. (f) Carbon particles consist of few-layer graphene.

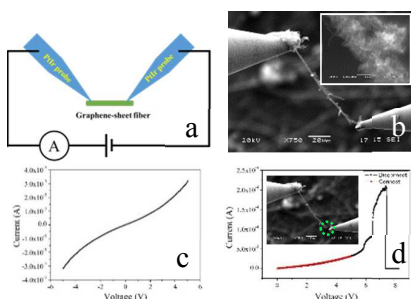


Figure 4 Electrical properties of individual GSF. (a) Setup of two-probe method in SEM equipment. (b) SEM image of the measured fiber. Inset: Enlarged SEM image. (c) I - V curve obtained at the bias voltage range of -5 to 5 V. (d) The maximum current and stability of the GSF. Inset: SEM image of disconnected GSF from electrode probe, in which the area was denoted by a green dotted ring.

substrate. Most importantly, the conversion process of coffee grounds into nanocarbons involves the production and exhaustion of some bio-gases, which can cause the vibration of the deposition pressure. Maybe because of this, the long GSFs have been generated in this process.

To investigate the electrical conductivity, two-probe technique (Figure 4a) was carried out in the vacuum chamber of SEM equipment (JSM-5600), in which one PtIr probe touched a fiber, then pulled it from the substrate, and another PtIr probe contacted the end of the fiber (Figure 4b). To ensure good electrical contact, i.e. Ohmic contact, between our sample and probe electrodes, several voltage sweeps of 0 - 5 V were applied to pass through this electrode-fiber-electrode circuit and to obtain the stable I - V curves. Although the I - V curves obtained with and without electron beam illumination indicated negligible difference, we still shut down the electron beam when taking the I - V curve expect for video tracking. Figure 4c presents the I - V curve obtained for an individual fiber with about 1.6 μm diameter and 92 μm length shown in Figure 4b. The I - V response clearly exhibits Ohmic contact in the lower voltage range, below 2 V, similar to graphene and carbon nanotubes. In a larger voltage range of -5 to 5 V, the I - V curve shows nonlinear symmetric behavior and an obvious conduction increase in a high-bias region. In the lower voltage, the resistance was calculated to be ~ 250 k Ω , which is comparable with those of carbon nanotubes.²⁹ We also checked the maximum current and stability of the sample by slowly increasing the applied bias voltage. As shown in Figure 4d, the fiber finally broke near the right-hand PtIr probe (inset of Figure 4d) at 7.4 V with a current of 200 μA . The results of in-situ SEM measurements of I - V curves present that the GSFs exhibited excellent conductivity, similar to most of carbon nanotubes.^{29, 30}

Finally, we examined the electrochemical performance of our GSFs in 1 M KCl aqueous solution using three-electrode measurement. Figure 5a shows that all cyclic voltammetric (CV) responses exhibited a near rectangle shape even at a high scan rate of 0.5 V/s, meaning the good capacitive behaviours of GSF film.

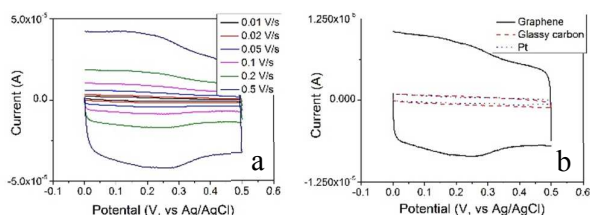


Figure 5 Electrochemical properties of the GSF film. (a) CV responses of graphene-modified electrode at various scan rates of 0.01 to 0.5 V/s with potential from 0 to 0.5 V in 1.0 M KCl. (b) CV curves of graphene-modified electrode, bare GC and Pt electrodes in 1.0 M KCl between 0 and 0.5 V with a scan rate of 0.1 V/s.

The areal capacitance at electrodes can be approximately evaluated from CV curves according to the following formula:

$$C_a = \frac{1}{S\nu(E_{ini} - E_{end})} \int_{E_{end}}^{E_{ini}} I(E)dE$$

, where C_a is the areal capacitance (F/cm^2), $I(E)$ is the response current (A), E_{ini} is the initial potential (V), E_{end} is the end potential (V), S is the surface area of the electrode (cm^2), and ν is the scan rate (V/s). Based on the CV curves (Figure 5b), the capacitance values are calculated to be 223.93 , 71.05 , and 1293.33 $\mu\text{F}/\text{cm}^2$ for bare Pt, glassy carbon (GC), and graphene-modified electrodes, respectively. Obviously, the GSF film has higher capacitance than the GC electrode. It may be due to special morphologies and microstructures of GSFs, which were confirmed above. Therefore, we speculate that the GSFs have potential applications in electrochemical conversion and storage devices.

Conclusions

We have demonstrated for the first time, the growth of GSFs from waste coffee grounds under the irradiation of microwave plasma of Ar and H_2 . The novel fibers not only possess special morphology and microstructure but also have relatively excellent electrical and electrochemical properties. Due to these advantages, the GSFs might be used in the fields of electrochemical energy conversion and storage. In addition, besides GSFs, other high-added-value graphene-based materials can be obtained from waste coffee grounds by MPI technique. Our approach is simple and effective, and it maybe stimulates another revolutionary of carbon science in sustainable energy technology.

Notes and references

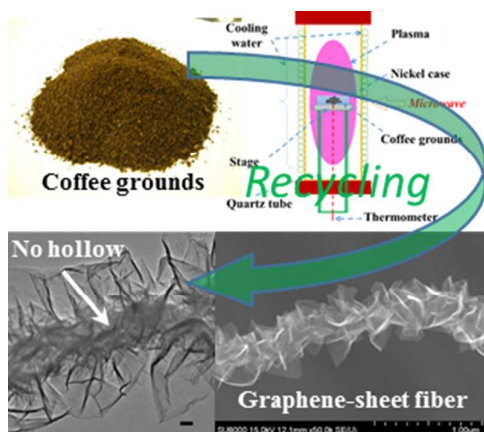
^aInstitute of Carbon Science and Technology, Shinshu University, 4-17-1 Wakasato, Nagano 380-8553, Japan. ^bDepartment of Electrical and Electronic Engineering, Shinshu University, 4-17-1 Wakasato, Nagano 380-8553, Japan. ^cDepartment of Chemical Science and Technology, Faculty of Bioscience and Applied chemical and Graduate School of Engineering, Hosei University, 3-7-2, Kajino-cho, Koganei, Tokyo184-8584, Japan. ^dResearch Center for Micro-Nano Technology, Hosei University, 3-11-15, Midori-cho, Koganei, Tokyo184-0003, Japan. ^eDepartment of Frontier Materials, Nagoya Institute of Technology, Gokiso-cho, Showa-ku, Nagoya 466-8555, Japan. ^fDepartment of Materials, Faculty of Mechanical Engineering, Universiti Teknologi Malaysia, 81310 Skudai, Johor, Malaysia. ^gDepartment of Physics, Department of Materials Science and Engineering & Materials Research Institute, The Pennsylvania State University, University Park, Pennsylvania 16802, United States. Tel: 81-26-2695670; E-mail: zp_wang@shinshu-u.ac.jp.

† Electronic Supplementary Information (ESI) available: Details of experimental section, SEM images, EDX patterns and TEM images. See DOI: 10.1039/x0xx00000x/

- 1 K. S. Novoselov, A. K. Geim, S. V. Morozov, D. Jiang, Y. Zhang, S. V. Dubonos, I. V. Grigorieva, A. A. Firsov, *Science* 2004, **306**, 666.
- 2 H. W. Kroto, J. R. Heath, S. C. O'Brien, R. F. Curl, R. E. Smalley, *Nature* 1985, **318**, 162.
- 3 S. Iijima, *Nature* 1991, **354**, 56.
- 4 H. Murayama, T. Maeda, *Nature* 1990, **345**, 791.
- 5 Y. Wu, P. Qiao, T. Chong, Z. Shen, *Adv. Mater.* 2002, **14**, 64.
- 6 K. Nakada, M. Fujita, G. Dresselhaus, M. S. Dresselhaus, *Phys. Rev. B* 1996, **54**, 17954.
- 7 D. V. Kosynkin, A. L. Higginbotham, A. Sinitskii, J. R. Lomeda, A. Dimiev, B. Katherine Price, J. M. Tour, *Nature* 2008, **458**, 872.
- 8 A. Oberlin, M. Endo, T. Koyama, *J. Cryst. Growth* 1976, **32**, 335.
- 9 K. S. Kim, Y. Zhao, H. Jang, S. Y. Lee, J. M. Kim, K. S. Kim, J.-H. Ahn, P. Kim, J.-Y. Choi, B. H. Hong, *Nature* 2008, **457**, 706.
- 10 X. Li, W. Cai, J. An, S. Kim, J. Nah, D. Yang, R. Piner, A. Velamakanni, I. Jung, E. Tutuc, S. K. Banerjee, L. Colombo, R. S. Ruff, *Science* 2009, **324**, 1312.

- 11 A. Reina, X. Jia, J. Ho, D. Nezich, H. Son, V. Bulovic, M. S. Dresselhaus, J. Kong, *Nano Lett.* 2009, **9**, 30.
- 12 L. C. Qin, D. Zhou, A. R. Krauss, D. M. Gruen, *Appl. Phys. Lett.* 1998, **72**, 3437.
- 13 J. Kim, M. Ishihara, Y. Koga, K. Tsugawa, M. Hasegawa, S. Iijima, *Appl. Phys. Lett.* 2011, **98**, 091502.
- 14 Y. Kim, W. Song, S. Y. Lee, C. Jeon, W. Jung, M. Kim, and C.-Y. Park, *Appl. Phys. Lett.* 2011, **98**, 263106.
- 15 J. J. Wang, M. Y. Zhu, R. A. Outlaw, X. Zhao, D. M. Manos, B. C. Holloway, V. P. Mammana, *Appl. Phys. Lett.* 2004, **85**, 1265.
- 16 Z. Wang, M. Shoji, H. Ogata, *Appl. Surf. Sci.* 2011, **257**, 9082.
- 17 D. H. Seo, Z. J. Han, S. Kumar, K. Ostrikov, *Adv. Energy Mater.* 2013, **3**, 1316.
- 18 D. H. Seo, S. Yick, S. Pineda, D. Su, G. Wang, Z. J. Han, K. Ostrikov, *ACS Sustainable Chem. Eng.* 2015, **3**, 544.
- 19 D. H. Seo, A. E. Rider, S. Kumar, L. K. Randeniya, K. Ostrikov, *Carbon* 2013, **60**, 211.
- 20 D. H. Seo, S. Pineda, S. Yick, J. Bell, Z. J. Han, K. Ostrikov, *Green Chem.* 2015, **17**, 2164.
- 21 Z. Wang, M. Shoji, K. Baba, T. Ito, H. Ogata, *Carbon* 2014, **67**, 326.
- 22 B. R. Stoner, A. S. Raut, B. Brown, C. B. Parker, J. T. Glass, *Appl. Phys. Lett.* 2011, **99**, 183104.
- 23 W. Yuan, Y. Zhou, Y. Li, C. Li, H. Peng, J. Zhang, Z. Liu, L. Dai, G. Shi, *Sci. Rep.* 2013, **3**, 2248.
- 24 L. M. Malard, M. A. Pimenta, G. Dresselhaus, M. S. Dresselhaus, *Phys. Rep.* 2009, **473**, 51.
- 25 J. Chopin, A. Kudrolli, *Phys. Rev. Lett.* 2013, **111**, 174302.
- 26 Z. Wang, H. Ogata, S. Morimoto, J. Ortiz-Medina, M. Fujishige, K. Takeuchi, H. Muramatsu, T. Hayashi, M. Terrones, Y. Hashimoto, M. Endo, unpublished.
- 27 Z. Wang, H. Ogata, S. Morimoto, M. Fujishige, K. Takeuchi, Y. Hashimoto, M. Endo, *Carbon* 2014, **72**, 421.
- 28 D. Mata, M. Ferro, A. J. S. Fernandes, M. Amaral, F. J. Oliveira, P. M. F. J. Costa, R. F. Silva, *Carbon* 2010, **48**, 2839.
- 29 D. Golberg, P. M. F. J. Costa, M. Mitome, Y. Bando, *Nano Res.* 2008, **1**, 166.
- 30 Q. Liu, W. Ren, Z.-G. Chen, L. Yin, F. Li, H. Cong, H.-M. Cheng, *Carbon* 2009, **47**, 731.

The table of contents entry



Microwave plasma-induced graphene-sheet fibers from waste coffee grounds show potential applications for electrochemical conversion and storage with excellent performances.